ELSEVIER

Biophysical Chemistry 63 (1997) 221–239

Biophysical Chemistry

Modelling the interrelations between calcium oscillations and ER membrane potential oscillations

Marko Marhl [a,b,*], Stefan Schuster [a], Milan Brumen [b,c], Reinhart Heinrich [a]

[a] *Theoretical Biophysics, Institute for Biology, Humboldt University, Invalidenstrasse 42, D-10115 Berlin, Germany*
[b] *Dept. of Physics, Faculty of Education, University of Maribor, Koroška cesta 160, SI-2000 Maribor, Slovenia*
[c] *J. Stefan Institute, Jamova 39, SI-1000 Ljubljana, Slovenia*

Received 31 July 1996; accepted 16 October 1996

Abstract

A refined electrochemical model accounting for intracellular calcium oscillations and their interrelations with oscillations of the potential difference across the membrane of the endoplasmic reticulum (ER) or other intracellular calcium stores is established. The ATP dependent uptake of Ca^{2+} from the cytosol into the ER, the Ca^{2+} release from the ER through channels following a calcium-induced calcium release mechanism, and a potential-dependent Ca^{2+} leak flux out of the ER are included in the model and described by plausible rate laws. The binding of calcium to specific proteins such as calmodulin is taken into account. The quasi-electroneutrality condition allows us to express the transmembrane potential in terms of the concentrations of cytosolic calcium and free binding sites on proteins, which are the two independent variables of the model. We include monovalent ions in the model, because they make up a considerable portion in the balance of electroneutrality. As the permeability of the endoplasmic membrane for these ions is much higher than that for calcium ions, we assume the former to be in Nernst equilibrium. A stability analysis of the steady-state solutions (which are unique or multiple depending on parameter values) is carried out and the Hopf bifurcation leading from stable steady states to self-sustained oscillations is analysed with the help of appropriate mathematical techniques. The oscillations obtained by numerical integration exhibit the typical spike-like shape found in experiments and reasonable values of frequency and amplitude. The model describes the process of switching between stationary and pulsatile regimes as well as changes in oscillation frequency upon parameter changes. It turns out that calcium oscillations can arise without a permanent influx of calcium into the cell, when a calcium-buffering system such as calmodulin is included. © 1997 Elsevier Science B.V.

Keywords: Calcium oscillation; Calcium-induced calcium release; Endoplasmic reticulum; ER transmembrane potential; Frequency encoding; Hopf bifurcation

1. Introduction

Oscillations of the cytosolic calcium concentration have attracted an ever increasing attention from experimentalists [1–6] and theoreticians [7–15]. Calcium oscillations in the form of repetitive spikes may be

* Corresponding author. Fax: +386-62-28180; e-mail: marko.marhl@uni-mb.si.

PII S0301-4622(96)02248-X

stimulated by hormones or neurotransmitters in hepatocytes, oocytes, cardiomyocytes, fibroblasts and many other cells, with the oscillation period ranging from seconds to minutes. It is now widely accepted that in a variety of cells, the oscillatory mechanism is closely related to the autocatalytic mobilization of calcium from the endoplasmic or sarcoplasmic reticulum [3,7,9,15]. This mechanism is called calcium-induced calcium release (CICR). It has been detected to occur in mitochondria also [6]. Often, further secondary messengers such as inositol 1,4,5-trisphosphate (IP_3) are involved.

The physiological significance of calcium oscillations includes the regulation of cell excretion, muscle contraction, activation of mammalian oocytes, cell signalling and other cellular activities [4,5,7]. In some instances, the function is still unknown. A number of putative biological advantages of oscillatory regimes of signalling in comparison to adjustable stationary messenger concentrations have been discussed in the literature. Cells usually maintain a low level of calcium. It is likely that larger concentrations of this ion somehow cause harm to the cell. This may be related to the fact that calcium is a bivalent ion. The Schulze–Hardy rule says that the critical concentrations for mono- and divalent counterions where coagulation of a colloid occurs is in the ratio 50:1 (cf., [16]). The problem of overloading the cell with calcium in the process of signalling can be overcome by usage of oscillatory mechanisms [3]. Another advantage is that a pulsatile signal can carry two types of information: a digital information (oscillation or stationarity) which acts as a switch (e.g., from glycogen synthesis to glycogenolysis), and an analogue signal which may determine the rate of some process (e.g., glycogenolysis) [5]. Oscillatory regimes are likely to allow rapid spatial propagation of signals [15]. Moreover, protein phosphorylation may be regulated more finely by oscillations since calmodulin and other calcium-binding proteins which regulate protein phosphorylation respond non-linearly with respect to free calcium [5]. In general, oscillations are believed to be a means to couple processes of different time-scales in the cell, for example fast electrophysiological processes to slower biochemical processes.

In a pioneering model for calcium oscillations proposed by Meyer and Stryer [17,18], oscillations result from a positive feedback loop between cytosolic calcium and the formation of IP_3. The oscillating variables are the concentrations of IP_3 and of cytosolic and stored calcium. Dupont and Goldbeter [14,19] developed a two-variable model based on the CICR mechanism, where the IP_3 concentration is considered as a parameter (cf. [7,9,15]).

Recently, attention has been drawn to the fact that oscillations of calcium are closely linked to oscillations of the electric potential difference across the endoplasmic or sarcoplasmic membrane, so that adequate modelling of this phenomenon should include electrochemical aspects [11,20]. In the cited works, the buffering by cytosolic calcium binding proteins is taken into account in extension to earlier models. The cytosolic calcium, the free calcium binding sites of proteins, the transmembrane potential of the endoplasmic reticulum (ER) and (only in the refined model [11]) the concentration of positive counterions are the model variables. The calcium concentration inside the ER is assumed to be constant.

In the present paper, we propose a refined electrochemical model for calcium oscillations. An essential new element of our model is the inclusion of monovalent anions such as chloride. They make up a considerable portion in the balance of electric charges. As the permeability of the endoplasmic membrane for small ions is much higher than that for calcium ions [21,22], we assume the monovalent anions as well as the monovalent cations such as potassium and sodium to be in Nernst equilibrium. As shown experimentally, potassium ions move into the ER upon release of calcium from the ER [23]. Furthermore, we take into account a leak flux of calcium out of the ER, in addition to the channel flux. In order to keep the dimension of the differential equation system small, we make use of the quasi-electroneutrality approximation. This method has been frequently used in the modelling of ion distribution in the presence of electric fields [24–27], but to our knowledge not yet in the modelling of calcium oscillations. It is based on the fact that very small net differences between cations and anions within the compartments are accompanied by a potential difference across the membrane in the observed order of magnitude. Moreover, in our model, we consider the calcium concentration inside the ER to be a variable linked with the cytosolic concentration by a conservation relation because the luminal volume of the ER is usually smaller than the volume of the cytoplasm.

The rate equations for the ion channels operating according to the calcium-induced calcium release mechanism and for the Ca^{2+}-ATPase are similar to those used in earlier models. The model also takes into account the binding of calcium to specific proteins such as calmodulin. Our model assumptions are related to those of a model describing the pH difference and transmembrane potential across membranes with electrogenic proton transport, such as mitochondrial membranes [28]. As regards the ER membrane, the primary electrogenic flux is that of calcium instead of protons. Both types of ions bind to proteins.

In Section 2 of this paper, we describe the basic assumptions and equations of the model. Section 3 is devoted to finding the steady states and determining their stability properties. The bifurcation leading from stable steady states to oscillations (Hopf bifurcation) is studied. In Section 4, results of numerical integration of the differential equations are presented. The effects of changes in the parameter values are discussed.

2. Basic model assumptions

The model system consists of a cell with an endoplasmic reticulum functioning as an internal calcium store. The model should be applicable to other organelles such as mitochondria after slight modification. We focus on the ion exchange between the cytoplasm and the calcium store, and we neglect the ion exchange between the cell and the extracellular medium. Because Ca^{2+} is actively transported by a specific pump, the Ca^{2+} exchange across the membrane is of central importance. Three types of Ca^{2+} fluxes are included in the model: (a) the ATP dependent uptake of Ca^{2+} from the cytosol into the ER, (b) the Ca^{2+} release from the lumen of the ER through channels following a CICR mechanism, and (c) a potential-dependent Ca^{2+} leak flux from the ER into the cytosol. Because of a high permeability of the ER membrane for most small ions except Ca^{2+} [21,22], not only Ca^{2+} fluxes are taken into account but also fluxes of monovalent cations and anions present in the cell. Moreover, the binding of calcium to proteins (Pr) in the cytosol is included. The entire model is schematically presented in Fig. 1.

The equation for the kinetics of calcium binding to proteins in the cytosol is given by:

$$\frac{\mathrm{d}Pr}{\mathrm{d}t} = k_{-}CaPr - k_{+}Ca_{\mathrm{cyt}}Pr \tag{1}$$

where Pr is the concentration of free protein calcium binding sites, Ca_{cyt} is the cytosolic calcium concentration, k_{+} and k_{-} are the on and off rate constants of the binding and dissociation, respectively. Note that $CaPr = Pr_{\mathrm{tot}} - Pr$, where Pr_{tot} is the total amount of protein calcium binding sites in the cell.

The time dependence of the cytosolic calcium concentration Ca_{cyt} is made up by the fluxes across the ER membrane and by the Ca^{2+} binding to proteins. Thus, the following equation can be written:

$$\frac{\mathrm{d}Ca_{\mathrm{cyt}}}{\mathrm{d}t} = J_{\mathrm{ch}} - J_{\mathrm{pump}} + J_{\mathrm{leak}} + k_{-}(Pr_{\mathrm{tot}} - Pr) - k_{+}Ca_{\mathrm{cyt}}Pr \tag{2}$$

Note that the fluxes are here taken to express the changes of mol per time and volume (rather than per time and surface).

We define the potential difference, $\Delta\psi$, as the electric potential in the cytosol minus that in the ER lumen:

$$\Delta\psi = \psi_{\mathrm{cyt}} - \psi_{\mathrm{ER}} \tag{3}$$

Owing to the presence of impermeable proteins in the cytosol and the operation of calcium pumps, $\Delta\psi$ is negative.

The reversal potential for calcium, E_{Ca}, is calculated by using the Nernst equation:

$$E_{\mathrm{Ca}} = \frac{RT}{2F}\ln\left(\frac{Ca_{\mathrm{ER}}}{Ca_{\mathrm{cyt}}}\right) \tag{4}$$

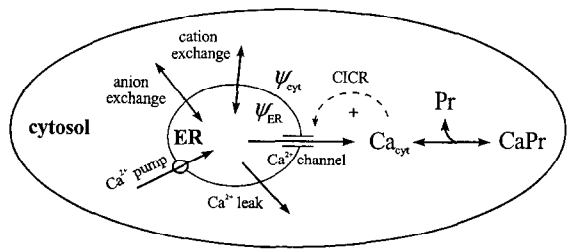

Fig. 1. Schematic presentation of the model system.

where R is the gas constant and T is the absolute temperature. E_{Ca} is the (hypothetical) potential which would arise if the actual calcium concentrations were in equilibrium.

The flux through the channels, J_{ch}, is given by:

$$J_{ch} = \kappa_{ch}(E_{Ca} - \Delta\psi) \tag{5}$$

The quantity κ_{ch} (with dimension $\mu MV^{-1}\ s^{-1}$) can be expressed as

$$\kappa_{ch} = \frac{g_{Ca}}{2FV_{cyt}} \tag{6}$$

where V_{cyt} denotes the cytosolic compartment volume, g_{Ca} is the ER membrane calcium conductance, and F is the Faraday constant. Eq. (5) is a minimalist equation describing the dependence of an ion flux on the transmembrane potential difference. It is derived from Ohm's law and has also been used by other authors [20,29,30]. More sophisticated equations describing this relationship are the Butler–Volmer equation (cf. [31]) and Goldman's flux equation [32,33].

The two calcium concentrations Ca_{cyt} and Ca_{ER} are linked by the conservation equation for calcium in the cell:

$$Ca_{tot} = Ca_{cyt} + \rho Ca_{ER} + (Pr_{tot} - Pr) \tag{7}$$

where ρ is the ratio between the ER volume and the cytosolic compartment volume.

The conductance of the channel is influenced by a cooperative binding of Ca^{2+} ions to the channel protein, as can be described by the Hill equation with a Hill coefficient of 2 [20]:

$$g_{Ca} = \frac{\tilde{g}_{Ca} S \left(\frac{Ca_{cyt}}{K_{Ca}}\right)^2}{1 + \left(\frac{Ca_{cyt}}{K_{Ca}}\right)^2} \tag{8}$$

where $\tilde{g}_{Ca}$ is the maximal ER membrane conductance per unit area, and S is the ER surface area. The half-saturation constant for calcium is denoted by K_{Ca}.

For simplicity's sake, the calcium transporting ATPase flux J_{pump} into the ER lumen is described by a linear dependence on Ca_{cyt}, because the pump was shown experimentally to operate in vivo on the linear part of the Michaelis–Menten curve (cf. [20]),

$$J_{pump} = k_{pump} Ca_{cyt} \tag{9}$$

where k_{pump} is the rate constant of ATPase.

In addition to earlier models, a leak flux out of the ER lumen dependent on the ER membrane potential difference is included. It can be described by:

$$J_{leak} = \kappa_{leak}(E_{Ca} - \Delta\psi) \tag{10}$$

Note that the parameter κ_{leak} (with dimension $\mu MV^{-1}\ s^{-1}$) is assumed to be constant, while the quantity g_{Ca} in Eq. (6) depends on the cytosolic Ca^{2+} concentration.

The electroneutrality condition [25–27] has to be valid in both model compartments separately, i.e., in the cytosol and in the ER lumen. Let us write this condition for the cytosol:

$$C_{cyt} - A_{cyt} + 2Ca_{cyt} - 2Pr = 0 \tag{11}$$

where C_{cyt} is the cytosolic concentration of monovalent cations (such as sodium and potassium) and A_{cyt} is the cytosolic concentration of monovalent anions (such as chloride). Because of a high permeability of the ER membrane for small ions other than Ca^{2+}, the cations and anions included in the model can be assumed to be in Nernst equilibrium:

$$\frac{C_{ER}}{C_{cyt}} = \frac{A_{cyt}}{A_{ER}} = \exp\left(\frac{F\Delta\psi}{RT}\right) \tag{12}$$

Because any exchange of ions with the extracellular medium is neglected, the cation (anion) concentration in the cytosol and the cation (anion) concentration in the ER obey, in addition to Eq. (12), the conservation relations:

$$C_{tot} = C_{cyt} + \rho C_{ER} \tag{13a}$$

$$A_{tot} = A_{cyt} + \rho A_{ER} \tag{13b}$$

where C_{tot} and A_{tot} are the total cation and anion concentrations, respectively, in the cell. Eq. (12), Eq. (13a) and Eq. (13b) imply

$$C_{cyt} = \frac{C_{tot}}{1 + \rho\exp\left(\frac{F\Delta\psi}{RT}\right)} \tag{14a}$$

$$A_{cyt} = \frac{A_{tot}}{1 + \rho\exp\left(-\frac{F\Delta\psi}{RT}\right)} \tag{14b}$$

Using the electroneutrality condition (Eq. (11)) for the cytosol and Eq. (14a) and Eq. (14b), $\Delta\psi$ can be expressed in terms of the other two model variables, Ca_{cyt} and Pr,

$$\Delta\psi = \frac{RT}{F}\ln\left(\frac{-b - \sqrt{b^2 - 4ac}}{2a}\right) \tag{15}$$

where

$$a = \rho(2Ca_{cyt} - 2Pr - A_{tot}) \tag{16}$$

$$b = C_{tot} - A_{tot} + 2(Ca_{cyt} - Pr)(1 + \rho^2) \tag{17}$$

and

$$c = \rho(2Ca_{cyt} - 2Pr + C_{tot}) \tag{18}$$

Eq. (15) is a solution of a quadratic equation and has been chosen so that the argument of the logarithmic function is positive, under consideration that a is negative.

Electroneutrality has to be valid also for the temporal changes of concentrations (cf. Eq. (11)):

$$\frac{dC_{cyt}}{dt} - \frac{dA_{cyt}}{dt} + 2\left(\frac{dCa_{cyt}}{dt} - \frac{dPr}{dt}\right) = 0 \tag{19}$$

which can be written as:

$$\frac{d(\Delta\psi)}{dt}\left(\frac{dC_{cyt}}{d(\Delta\psi)} - \frac{dA_{cyt}}{d(\Delta\psi)}\right) + 2\left(\frac{dCa_{cyt}}{dt} - \frac{dPr}{dt}\right) = 0 \tag{20}$$

Taking Eq. (1), Eq. (2), Eq. (14a) and Eq. (14b) into account the following expression for

$$d(\Delta\psi)/dt$$

is obtained from Eq. (20):

$$\frac{d(\Delta\psi)}{dt} = \frac{2RT(J_{ch} - J_{pump} + J_{leak})}{\rho F\left[C_{tot}\exp\left(\frac{F\Delta\psi}{RT}\right)/\left[1+\rho\exp\left(\frac{F\Delta\psi}{RT}\right)\right]^2 + A_{tot}\exp\left(-\frac{F\Delta\psi}{RT}\right)/\left[1+\rho\exp\left(-\frac{F\Delta\psi}{RT}\right)\right]^2\right]} \tag{21}$$

This equation is the differential form of the model Eq. (15). It is not directly used in our calculations since we have been able to derive $\Delta\psi$ as an explicit function of the other system variables, that is, Ca_{cyt} and Pr. Nevertheless, the differential form of the electroneutrality condition is much more useful in general. For example, Eq. (11) expressing electroneutrality may not be solved for $\Delta\psi$ so easily as a function of Ca_{cyt} and Pr in other situations, e.g., if it were of higher order with respect to $\Delta\psi$. In this way the equation in the differential form would be preferable in general (see [27]).

Our model involves three main variables (Ca^{2+} concentration in the cytosol Ca_{cyt}, concentration of free proteins Pr, and potential difference $\Delta\psi$ across the ER membrane). All other model variables can be easily expressed in terms of Ca_{cyt}, Pr, and $\Delta\psi$. In fact, C_{cyt} and A_{cyt} can be calculated from Eq. (14a) and Eq. (14b), C_{ER} and A_{ER} from Eq. (13a) and Eq. (13b), $CaPr$ is simply $Pr_{tot} - Pr$, and Ca_{ER} follows from Eq. (7). Note that $\Delta\psi$ is an explicit function of Ca_{cyt} and Pr (Eq. (15)) which means that our model system is actually two-dimensional. However, for purely technical reasons (see Section 3) we preserve three model equations which can be considered as an algebro-differential equation system consisting of two differential equations (Eq. (1) and Eq. (2)) and one algebraic equation (Eq. (15)). Anyway, in the framework of dynamical systems theory the trajectory of the considered system is restricted to a two-dimensional manifold.

The model parameters used in our calculations are listed in Table 1. The values for V_{cyt} and S are taken for a concrete biological system (*Xenopus* oocytes) studied by Jafri et al. [20]. All other values are not directly related to a specific cell. In view of a general mathematical model average values from different sources are taken where similar systems have been considered. So the value for Ca_{tot} is set to 45 μM, because values of 2 μM [13], 15 μM [11] and values up to the millimolar range [20,22] were reported. The half-saturation constant for calcium K_{Ca} can be conceived of as a dissociation constant of calcium from the channel protein. We take it in accordance to the values used by Standen and Stanfield [34] and Jafri et al. [20]. The conductance $\tilde{g}_{Ca}$ is in agreement to the experimental data for single channel conductivity [30] extrapolated to low calcium concentrations and reported values of the channel density in the membrane [35]. For the rate constants k_+ and k_- of the binding to, and dissociation from the proteins, respectively, we use similar values as Jafri and coworkers [11,20]. Recent experimental observations suggest that these values are higher [36]. However, we believe that the finite velocity of diffusion of calcium ions through the cytoplasm should be taken into account. This diffusion causes a sort of delay which may be modelled by using smaller values of the rate constants k_+ and k_-, which are then to be regarded as effective parameters. This argument can be illustrated by the reasoning that

Table 1
The model parameters for the reference case [a,b]

Parameter	Value
Geometrical parameters	
V_{cyt}	5.84×10^{-11} l
S	6.16×10^{-3} cm^2
ρ	0.01
Conservation sums	
C_{tot}	5×10^{3} μM
A_{tot}	3.89×10^{3} μM
Ca_{tot}	45 μM
Pr_{tot}	600 μM
Kinetic parameters	
K_{Ca}	5 μM
k_-	0.5 s^{-1}
k_+	0.1 μM^{-1} s^{-1}
$\tilde{g}_{Ca}$	100 μS cm^{-2}
k_{pump}	76 s^{-1}
κ_{leak}	10.0 μM V^{-1} s^{-1}

[a] All results are calculated for these parameters unless otherwise stated.
[b] Note that the conservation sums fulfil the electroneutrality condition for the whole cell. In Fig. 2 and Fig. 3, k_{pump} is varied and in Fig. 4, Fig. 6 and Fig. 8, both k_{pump} and $\tilde{g}_{Ca}$ are varied.

high values of the rate constants allow one to employ a rapid buffering approximation near the point sources of calcium (cf. [36]). If this approximation were applied to the whole cytosol, it would lead to a reduction of the effective dimension of the differential equation system to one, so that oscillations would be excluded.

3. Steady states and stability

As usual in the analysis of a dynamical system, important steps are the determination of steady states and their stability. The above-mentioned fact that the dynamical system under study is essentially two-dimensional simplifies this procedure considerably. If the two differential Eq. (1) and Eq. (2) are rewritten in the following form:

$$\frac{dCa_{cyt}}{dt} = f_1\left(Ca_{cyt}, Pr, \Delta\psi\left(Ca_{cyt}, Pr\right)\right) \tag{22}$$

$$\frac{dPr}{dt} = f_2\left(Ca_{cyt}, Pr, \Delta\psi\left(Ca_{cyt}, Pr\right)\right) \tag{23}$$

the steady-state condition can be expressed as:

$$f_1 = 0 \tag{24a}$$

$$f_2 = 0 \tag{24b}$$

For any given set of model parameters, solving Eq. (24a), Eq. (24b) and Eq. (15) simultaneously gives the steady state values $\overline{Ca}_{cyt}$, $\overline{Pr}$, and $\overline{\Delta\psi}$ of the main model variables. An analytical calculation of these values is not straightforward because the model variables enter the equations in a non-linear way. To achieve a semi-analytical treatment in solving these equations it is convenient to formally consider one actual variable to be known and some model parameter as a function of this variable, thus exchanging, for purely technical

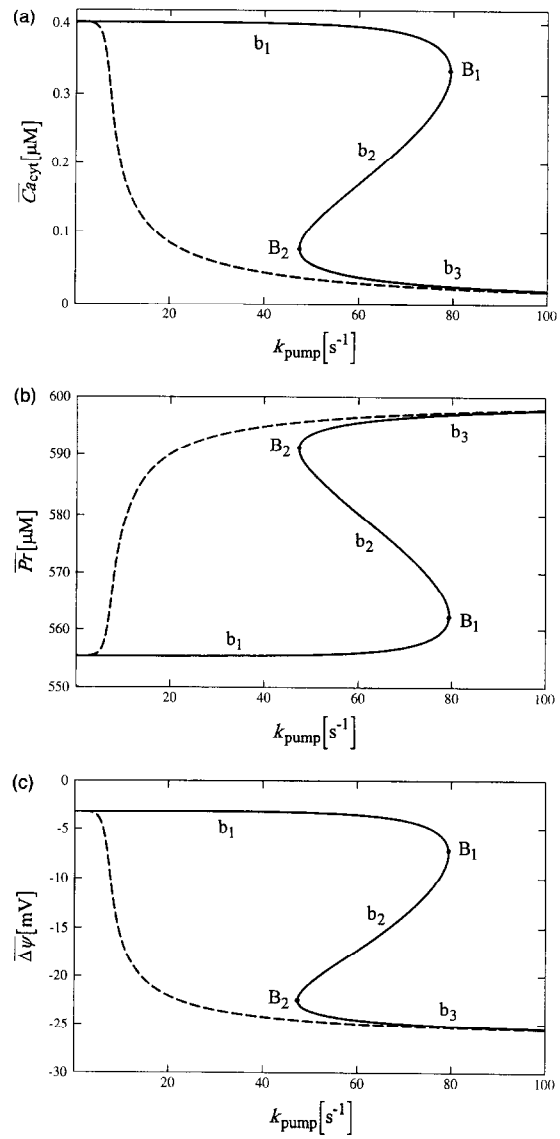

Fig. 2. Steady-state values $\overline{Ca}_{cyt}$ (A), $\overline{Pr}$ (B), and $\overline{\Delta\psi}$ (C) in dependence on the parameter k_{pump}. The conductivity $\tilde{g}_{Ca}$ has the values 100 μS cm^{-2} (solid curves) and 5 μS cm^{-2} (dashed curves). For the other parameters see Table 1. The symbols B_1 and B_2 are used for turning points where the number of steady states changes, and the branches of the curve are denoted by b_1, b_2, and b_3.

reasons, the roles of a variable and a parameter. In our calculations, we choose $\overline{Ca}_{cyt}$ and k_{pump}. The following procedure is used: (a) some $\overline{Ca}_{cyt}$ value is prescribed, (b) from Eq. (24b) the corresponding value for $\overline{Pr}$ is calculated, (c) from Eq. (15) the value for $\overline{\Delta\psi}$ is determined, and (d) from Eq. (24a) the value for k_{pump} is calculated. This procedure is consecutively repeated for other values of $\overline{Ca}_{cyt}$ in a given interval. This gives a plot of all model variables versus the parameter k_{pump} which is represented on the abscissa. For the model parameters given in Table 1 these dependencies are shown in Fig. 2.

It is seen that for low values of the conductivity $\tilde{g}_{Ca}$, the steady-state solution for $\overline{Ca}_{cyt}$, $\overline{Pr}$, and $\overline{\Delta\psi}$ is unique in the whole range of k_{pump} (dashed lines in Fig. 2). For higher values of $\tilde{g}_{Ca}$ the solution is, depending on the

parameter k_{pump}, either unique or it leads to three different steady states (solid lines in Fig. 2). In Fig. 2A–C, the points B_1 and B_2 represent the points where at variation of k_{pump} the number of steady states changes. They entail that the curves for high $\tilde{g}_{Ca}$ consist of three parts, denoted by b_1, b_2, and b_3. For all values of k_{pump} smaller than that corresponding to the point B_2, as well as for all values of k_{pump} larger than that corresponding to the point B_1 only one steady state exists. In contrast, between the points B_1 and B_2 three steady states can be found. In the case when $k_{leak} = 0$, i.e., when no Ca^{2+} leak flux from the ER into the cytosol is present, the curve branch b_3 is identical to a straight line which is given by $\overline{Ca}_{cyt} = 0$. According to Eq. (24b) and Eq. (15) it leads to $\overline{Pr} = Pr_{tot} = 600$ μM and $\overline{\Delta\psi} = -26.5$ mV.

For the calculated steady states a local stability analysis is performed. In the first step the Jacobian matrix is calculated:

$$\mathbf{J} = \begin{pmatrix} \dfrac{\partial f_1}{\partial Ca_{cyt}} & \dfrac{\partial f_1}{\partial Pr} \\ \dfrac{\partial f_2}{\partial Ca_{cyt}} & \dfrac{\partial f_2}{\partial Pr} \end{pmatrix} \tag{25}$$

All partial derivatives $\partial f_i/\partial Ca_{cyt}$ and $\partial f_i/\partial Pr$ for $i = 1,2$ can be calculated directly from Eq. (24a) and Eq. (24b) with substitution of $\Delta\psi$ from Eq. (15). However, we calculate them in a simpler way, as follows.

(a) The partial derivative $\partial f_1/\partial Ca_{cyt}$ can be rewritten by using the chain rule:

$$\frac{\partial f_1}{\partial Ca_{cyt}} = \frac{\partial}{\partial Ca_{cyt}} f_1\big(Ca_{cyt}, Pr, \Delta\psi(Ca_{cyt}, Pr)\big) = \frac{\partial f_1}{\partial Ca_{cyt}}\Big|_{\Delta\psi} + \frac{\partial f_1}{\partial(\Delta\psi)}\frac{\partial(\Delta\psi)}{\partial Ca_{cyt}} \tag{26}$$

where the expressions for $\partial f_1/\partial Ca_{cyt}|_{\Delta\psi}$ and $\partial f_1/\partial(\Delta\psi)$ can be derived directly from Eq. (22) and Eq. (24a). The symbol $|_{\Delta\psi}$ means that the derivative is taken at constant $\Delta\psi$. Note that in the derivatives entering the Jacobian matrix, $\Delta\psi$ must not be kept constant because it is coupled with the other two model variables by the algebraic constraint (Eq. (15)). The derivative $\partial(\Delta\psi)/\partial Ca_{cyt}$ which enters Eq. (26) may be calculated by using the electroneutrality condition. Let us rewrite Eq. (11) as:

$$h = C_{cyt} - A_{cyt} + 2Ca_{cyt} - 2Pr = 0 \tag{27}$$

The partial derivative $\partial h/\partial Ca_{cyt}$ can be expanded in an analogous way as $\partial f_1/\partial Ca_{cyt}$ in Eq. (26). Since $\partial h/\partial Ca_{cyt} = 0$, it follows that

$$\frac{\partial(\Delta\psi)}{\partial Ca_{cyt}} = -\frac{\dfrac{\partial h}{\partial Ca_{cyt}}\Big|_{\Delta\psi}}{\dfrac{\partial h}{\partial(\Delta\psi)}} \tag{28}$$

(b) An expression for the partial derivative $\partial f_1/\partial Pr$ can be derived analogously to the procedure given in step (a).

(c) Because f_2 is independent of $\Delta\psi$ the expressions for $\partial f_2/\partial Ca_{cyt}$ and $\partial f_2/\partial Pr$ can be derived directly from Eq. (23) and Eq. (24b).

The trace, tr, of the Jacobian, i.e., the sum of its diagonal elements, and the determinant, Δ, are of special interest in the stability analysis,

$$tr = \frac{\partial f_1}{\partial Ca_{cyt}} + \frac{\partial f_2}{\partial Pr} \tag{29}$$

$$\Delta = \frac{\partial f_1}{\partial Ca_{cyt}}\frac{\partial f_2}{\partial Pr} - \frac{\partial f_1}{\partial Pr}\frac{\partial f_2}{\partial Ca_{cyt}} \tag{30}$$

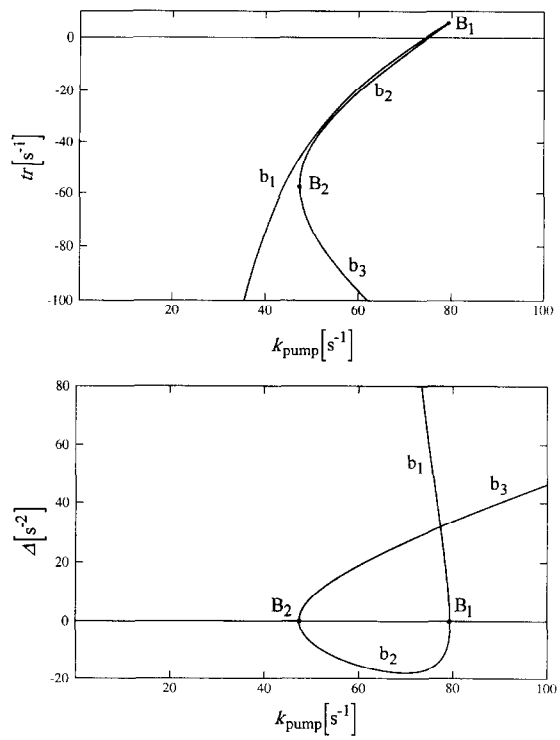

Fig. 3. Plot of the trace (A) and the determinant of the Jacobean (B) versus the rate constant of the Ca^{2+} pump.

Analysis of these quantities, in particular of their signs, allows one to distinguish between different types of steady states (stable node, unstable focus, etc.). For example, we can determine these types for the steady states shown in Fig. 2 in dependence on the parameter k_{pump}. To do so, we plot tr and Δ in dependence on k_{pump} (Fig. 3). To establish a correspondence between these figures the same notation for the branches b_1, b_2, and b_3 is used. In this way, we are now in a position to determine the stability properties of the steady states plotted in Fig. 2.

From Fig. 3 it is easy to see that the branch b_2 represents saddle points since $\Delta < 0$. For the whole branches b_1 and b_3 the relation $\Delta > 0$ holds true. Of special interest is a part of branch b_1 where $tr > 0$. There steady states are unstable, whereas all other steady states on branch b_1 and all steady states on b_3 are stable. A steady state is an unstable focus if $\Delta > 0$, $tr > 0$, and $tr^2 < 4\Delta$ (cf. [12,37]). In parameter ranges where these conditions are fulfilled, self-sustained oscillations are likely to occur. Such a range can be detected in Fig. 3. It is located on the branch b_1 in the neighbourhood of the point B_1. To show that in this parameter range self-sustained oscillations in the sense of limit cycles occur, numerical integration of the model equations is required, as will be presented in the following section.

To get more information about the system a stability analysis in the space of two model parameters is helpful. We use a plot of two curves determined by $tr = 0$ or $\Delta = 0$ in the plane spanned by k_{pump} and $\tilde{g}_{Ca}$ (Fig. 4). Note that this plot can be conceived of as a projection of curves where $tr = 0$ or $\Delta = 0$ on the surface determined by the stationary calcium concentration as a function of k_{pump} and $\tilde{g}_{Ca}$. The projection is made onto the plane spanned by these two parameters. The above-mentioned surface is folded because in the central region, three stationary states exist. This can be seen from Fig. 2, which is a cross-section of this surface for the fixed value of $\tilde{g}_{Ca} = 100\ \mu S\ cm^{-2}$ (solid lines). The curve $\Delta = 0$ corresponds to the turning points of this fold, which means that it separates regions with different numbers of steady states within the parameter space.

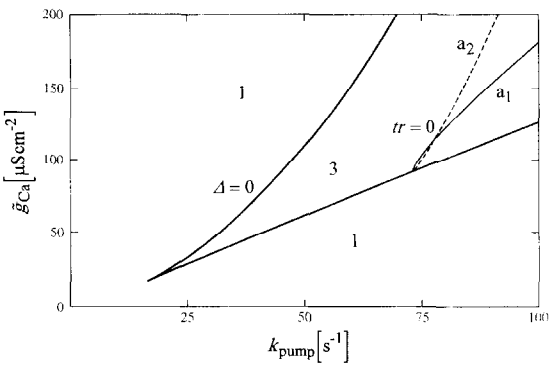

Fig. 4. The curves $tr = 0$ and $\Delta = 0$ in the parameter space of k_{pump} and $\tilde{g}_{Ca}$. The numbers 1 and 3 correspond to the numbers of steady states in the regions determined by the curve $\Delta = 0$. For the branch a_1 of the curve $tr = 0$ the relation $\Delta > 0$ holds true which means that it is the line of Hopf bifurcations. The curve branch a_2 (dashed curve) corresponds to $\Delta < 0$.

The curve $tr = 0$ corresponds to a Hopf bifurcation (cf. [15,37]), that is, a transition from an unstable focus to a stable focus or vice versa, provided that in addition, $\Delta > 0$ (branch a_1 in Fig. 4). Hopf bifurcations are supercritical or subcritical according to whether the amplitude of the limit cycle grows beginning with zero or with a finite value. Both types of bifurcation have been found in our model. Note that different types of bifurcations, as well as other specific behaviours of the model system, can be obtained by different sets of model parameters. From Fig. 4, it is seen that below a certain limit for $\tilde{g}_{Ca}$ no Hopf bifurcation can occur. For very low $\tilde{g}_{Ca}$ values, the model system has only one steady state in the whole region of k_{pump} values which leads to the dashed line in Fig. 2 (for $\tilde{g}_{Ca} = 5\ \mu S\ cm^{-2}$). The stability analysis gives us still more information about the system. Using another set of parameters, the curve $tr = 0$ in the parameter space of k_{pump} and $\tilde{g}_{Ca}$ can be situated, for example, partially outside the region where the system has three steady states (see below).

4. Numerical simulation of oscillations and model predictions

The local stability analysis gives us ranges for model parameters for which oscillations can be expected. To simulate the oscillations the model equations should be integrated. The results of numerical integration for the reference case are shown in Fig. 5. Our model reproduces a typical form of cytosolic calcium oscillations, i.e., the form of calcium spikes which have frequently been observed experimentally [1–4]. The potential difference $\Delta\psi$ across the ER membrane oscillates in phase with the calcium spikes. When the cytosolic calcium is increased, i.e., when calcium is released from the ER lumen into the cytosol, the ER membrane is depolarized and when the calcium is pumped back into the ER the membrane is repolarized. That is in agreement with the understanding of processes on the ER membrane [22]. Note that the shape of $\Delta\psi$ oscillations is very different from the form of Ca_{cyt} oscillations. It is much more similar to the oscillations of the free protein concentration in the cytosol. That shows that the time course of the potential difference is not directly related to the free Ca^{2+} concentration in the cytosol but rather to the total Ca^{2+} concentration in the cytosol, including that bound to proteins. The role of proteins is also shown by the different form of Ca_{cyt} oscillations and Ca_{ER} oscillations (compare Fig. 5A and D). We have not plotted the oscillations of the highly permeable monovalent ions because they are related with the $\Delta\psi$ oscillations via the Nernst equation (Eq. (12)) in a straightforward way.

One purpose of a mathematical model is to predict different effects when some model parameters are changed. In the case of oscillations, it is difficult to study independent effects of some model parameters. If one model parameter is changed the property of the steady-state solution to be an unstable focus often gets lost. Thus, a simultaneous change of other model parameters is required to preserve the self-sustained oscillations. In

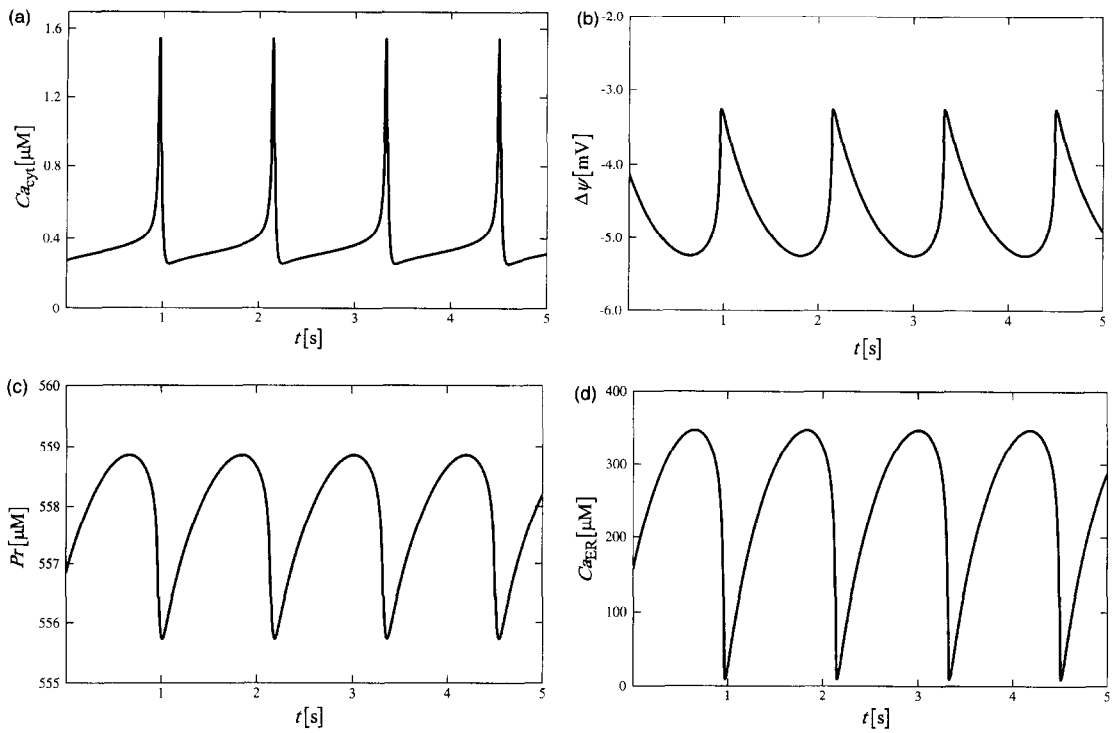

Fig. 5. Oscillations of the cytosolic calcium (A), the potential difference on the ER membrane (B), free proteins in the cytosol (C), and calcium in the ER (D) for the reference case (see Table 1 for model parameters).

Fig. 6, one can see that if the volume ratio ρ is increased by a factor of 10, the oscillations are not possible for the same parameters as in the reference case, in particular for $\tilde{g}_{Ca} = 100$ μS cm^{-2} (compare Fig. 4 and Fig. 6).

The volume ratio, ρ, is an important model parameter. Different cells have different volume ratios between the ER and the total cell volume. To our knowledge, this ratio is ranged between about 6% [20] and 15% [38]. Accordingly, if not only parts but the whole ER lumen are considered to have a function of calcium storage the

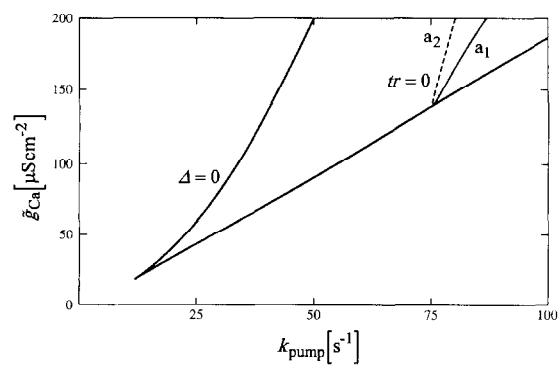

Fig. 6. The curves $tr = 0$ and $\Delta = 0$ in the parameter space of k_{pump} and $\tilde{g}_{Ca}$ for $\rho = 0.1$ (for the other parameters see Table 1). For the branch a_1 of the curve $tr = 0$ the relation $\Delta > 0$ holds true, so that it corresponds to Hopf bifurcations. The curve branch a_2 (dashed curve) corresponds to $\Delta < 0$.

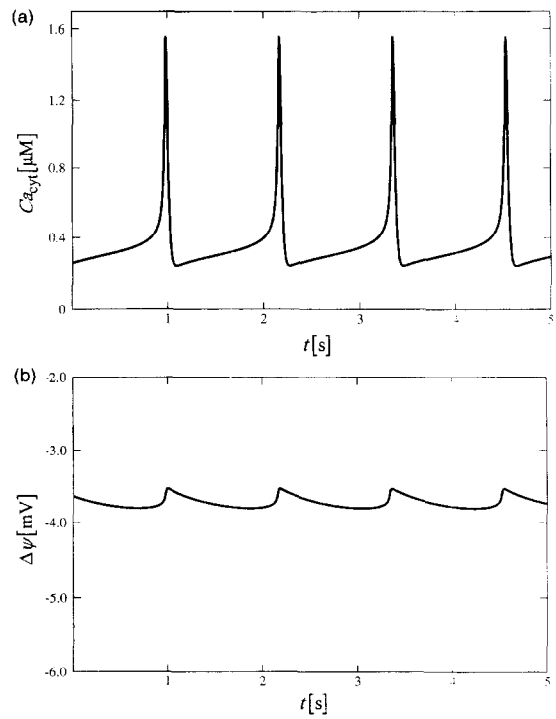

Fig. 7. Oscillations of the cytosolic calcium (A) and the potential difference across the ER membrane (B) for $\rho = 0.1$. Parameter values differing from those listed in Table 1: $\tilde{g}_{Ca} = 157\ \mu S\ cm^{-2}$, $k_{pump} = 80.8\ s^{-1}$.

model parameter ρ can be set to the value of about 10% (see Fig. 6 and Fig. 7). But because it is known that the ER is subdivided into rough and smooth portions (RER and SER, respectively) and that only the SER with its irregular network of smooth-surfaced tubules has a calcium regulation function [38] it seems to be more realistic to take a smaller value for ρ. An exact value is difficult to set because the ratio of RER/SER varies considerably among cells depending on the level of protein synthesis and other activities. Another reason to work with smaller values for ρ is that in addition to the SER and RER there are at least 4 other morphologically distinct domains of the ER including the nuclear envelope, transitional elements, crystalloid ER, and luminal ER bodies containing protein aggregates [38]. Therefore, ρ is set to 1% in the reference case of our model. The effects of changing the volume ratio are important for predicting the ER membrane potential variations during oscillations. From comparison of Fig. 5 and Fig. 7 it is evident that with the calcium spiking being about the same the potential oscillations are different. If the volume ratio is increased by a factor of 10 the amplitudes of the potential are smaller by approximately the same factor.

Note that the amplitudes of the potential are also strongly affected by counterion transport across the ER membrane. If in the model the total cation and anion concentrations are increased by a given factor it has an analogous effect as if the volume ratio were increased by the same factor (not shown here). This is fully in agreement with the experimental observations of Beeler et al. [21] showing that high ion fluxes through anion and cation channels in the ER membrane are sufficiently fast to neutralize potential changes which may take place during Ca^{2+} uptake or release.

In a given biological system, cytosolic calcium oscillations with different frequencies can occur [1,5]. The frequency depends on the intensity of calcium entry into the cytosol either from intracellular sources, usually through calcium release mediated by a second messenger, such as IP_3, or from extracellular sources through

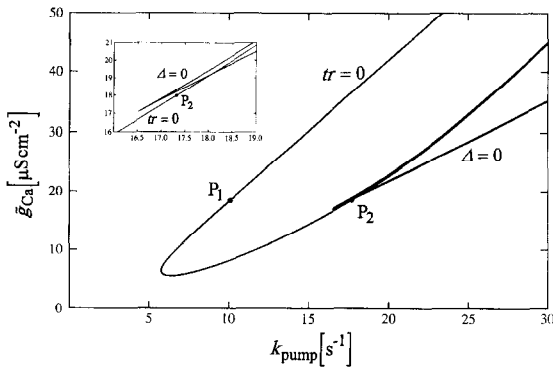

Fig. 8. The curves $tr = 0$ and $\Delta = 0$ in the parameter space of k_{pump} and $\tilde{g}_{Ca}$ for $k_- = 0.005\ s^{-1}$ and $k_+ = 0.001\ \mu M^{-1}\ s^{-1}$ (for the other parameters see Table 1). For the whole curve $tr = 0$ the relation $\Delta > 0$ holds true which means that it is the line of Hopf bifurcations. Points P_1 and P_2 represent a supercritical Hopf bifurcation and a subcritical Hopf bifurcation, respectively, for $\tilde{g}_{Ca} = 18\ \mu S\ cm^{-2}$. Inset: Amplification of part of the plot.

plasma membrane calcium channels. In our model, proteins in the cytosol can be seen as a second pool for calcium release and storage. Indeed, a change in protein affinity strongly affects the frequency of calcium oscillations (see below).

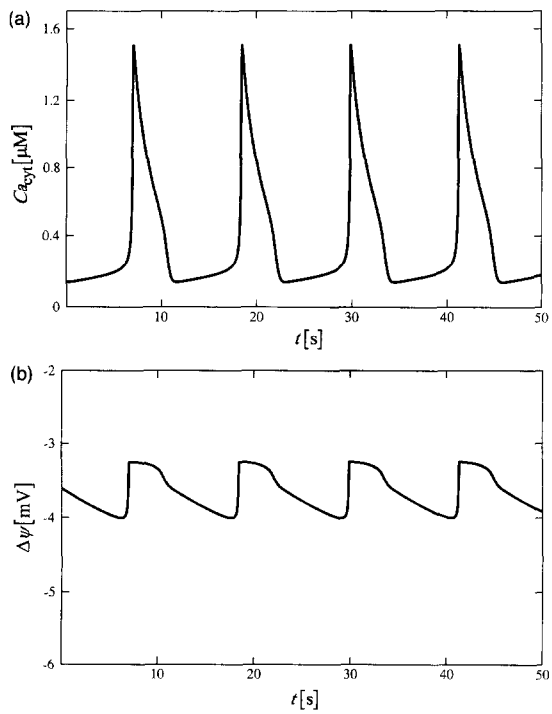

Fig. 9. Oscillations of the cytosolic calcium (A) and ER membrane potential (B) for $k_- = 0.005\ s^{-1}$, $k_+ = 0.001\ \mu M^{-1}\ s^{-1}$, $\tilde{g}_{Ca} = 18\ \mu S\ cm^{-2}$, and $k_{pump} = 11.5\ s^{-1}$.

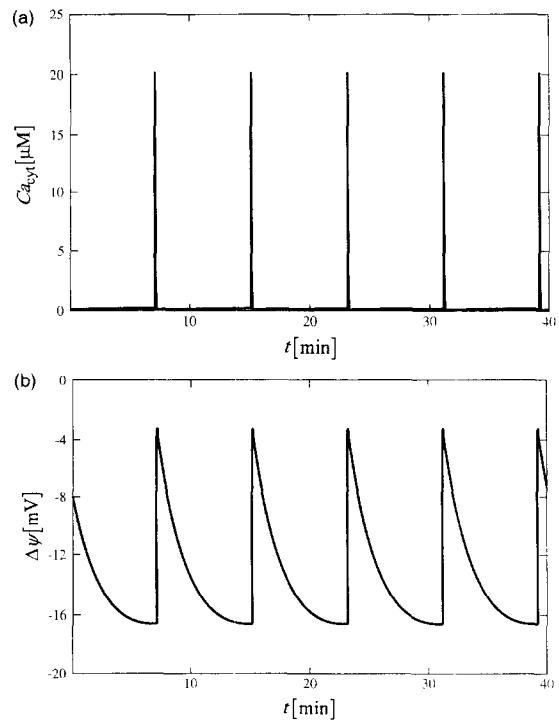

Fig. 10. Oscillations of the cytosolic calcium (A) and ER membrane potential (B) for $k_- = 0.005\ s^{-1}$, $k_+ = 0.001\ \mu M^{-1}\ s^{-1}$, $\tilde{g}_{Ca} = 18\ \mu S\ cm^{-2}$, and $k_{pump} = 17.33\ s^{-1}$.

As noted above it is not easy to study independent effects caused by the change of some model parameters. If in the model the rate constants of the binding and dissociation (k_+ and k_-, respectively) are decreased, for example, by a factor of 100 with respect to the reference case, at the same time also the maximal channel conductivity $\tilde{g}_{Ca}$ and the pump activity k_{pump} have to be changed to preserve the self-sustained oscillations (see Fig. 8).

In the amplified part of Fig. 8, it can be seen that the curve $\Delta = 0$ is in a particular range of the parameter space positioned inside the region $tr > 0$. Let us take $\tilde{g}_{Ca} = 18\ \mu S\ cm^{-2}$. The corresponding points on the curve $tr = 0$ are denoted by P_1 and P_2. In both cases $\Delta > 0$, which means that the points P_1 and P_2 correspond to Hopf bifurcations. For parameters taken in the neighbourhood of P_1 and P_2, where $tr > 0$, self-sustained oscillations are expected. Note that the neighbourhoods of the points P_1 and P_2 correspond to states with high and low steady-state Ca^{2+} concentrations, respectively, in the cytosol. This means that in the first case the oscillations occur around a steady state where most of the Ca^{2+} is contained in the cytosol bound to the proteins and in the second case the oscillations occur around a steady state where most of the Ca^{2+} is contained in the ER.

It has been found that the point P_1 represents a supercritical Hopf bifurcation and the point P_2 represents a subcritical Hopf bifurcation. This means that at the point P_1 the amplitude of the limit cycle grows beginning with zero and so in the neighbourhood of this point such a parameter k_{pump} can be found that the amplitude of cytosolic calcium oscillations is adjusted to that resulting for the reference values (see Fig. 9A and B for the corresponding ER membrane potential oscillations). In contrast, at the point P_2 the amplitudes of oscillations begin with a finite value and are, hence, rather insensitive against parameter variations in the neighbourhood of this point. The amplitudes are much larger than in the first case (see Fig. 10A and B). However, in both cases

the frequency of oscillations is considerably lowered with respect to the reference case as the constants k_+ and k_- are decreased.

5. Discussion

In the present paper, we have established an extended electrochemical model accounting for oscillations of intracellular calcium and the electric potential difference across the membrane of the endoplasmic reticulum. The model should be modifiable so that it can be applied to other intracellular calcium stores. It involves three types of calcium flux across the ER membrane: (a) the ATP-dependent uptake into the ER, (b) the release following a CICR mechanism, and (c) a potential-dependent, non-autocatalytic leak. This leak may flow across the lipid phase of the membrane as well as through calcium channels. We have included it because otherwise, the widely used rate equation for the CICR mechanism would imply that a trivial steady state occurs where the cytosolic calcium concentration is zero. Including a non-autocatalytic leak shifts this steady state to one with a very small, but non-zero concentration, which appears to be more realistic.

In the models of Jafri and coworkers [11,20], the capacitance equation was used to establish a differential equation for the transmembrane potential, which is of the form '$C_m S[d(\Delta\psi)/dt]$ = charge balance of ion fluxes', where C_m is the membrane capacitance per unit area. It is an experimentally observed fact that this quantity is very low in the sense that the term on the left-hand side of the above equation is small compared to the particular terms of the charge balance. Accordingly, a plausible simplification is achieved by considering the limit $C_m = 0$. This is a special case of the quasi-steady-state assumption (cf. [12]). In this limit, the differential equation in question leads to the electroneutrality condition for ion fluxes, which can be rewritten as a similar condition for ion concentrations. According to the capacitance equation, this means that a very small net electric charge difference across the membrane is accompanied by an electric potential difference counteracting any further separation of charges. The electroneutrality condition is an algebraic equation linking the transmembrane potential, $\Delta\psi$, to the concentrations of free calcium and proteins. The time course of these variables is governed by differential equations, from which the time course of $\Delta\psi$ can then be calculated. Doing so has the advantage that knowledge of the membrane capacitance is no longer necessary. Furthermore, the concomitant reduction in the dimension of the differential equation system simplifies the analytical treatment considerably (for example, in the stability analysis).

Elaborating on a proposal by Jafri and Gillo [11], we have included the effect of counterions. We have not only included positively charged counterions, but also anions since they contribute to the charge balance to about the same extent. In order to keep the dimension of the differential equation system small, we have renounced to include additional differential equations for the counterions and have applied, instead, the Nernst equation for these ions. This is a sort of rapid-equilibrium approximation, which is justified in this case because the membrane permeability for sodium, potassium, chloride and similar monovalent ions is much higher than that for calcium [21,22]. One of the advantages of this approach is that knowledge of the permeability for the counterions is not necessary. Whereas the model of Jafri and Gillo [11] gives rise to a permanent slow decrease in the cytosolic counterion concentration, which implies that the calcium oscillations are damped, our model yields undamped oscillations for appropriate parameter values.

The binding of calcium to proteins has turned out to be of essential importance in the generation of calcium oscillations. Since free calcium has a very low intracellular concentration, it does not contribute very much to the electroneutrality balance and would not, without this calcium buffering system, make possible remarkable changes in transmembrane potential. Interestingly, the finite velocity of the calcium binding to, and dissociation from, proteins is essential for the occurrence of oscillations. If this binding is assumed to be in rapid equilibrium, the effective dimension of the differential equation system reduces to one, so that oscillations are excluded. The low values for the rate constants of binding and dissociation used in our model are to be regarded as effective parameters also reflecting the diffusion of calcium through the cytosol.

In accordance with some earlier models [7,14,19], we considered the calcium concentration in the calcium stores to be variable. Since we neglected any flux through the plasmalemmal membrane, this concentration is linked with the cytosolic calcium concentration by a conservation relation and is not, hence, an independent variable. In some other models [11,20], this quantity was considered to be constant. That assumption is contestable because the volume of the calcium stores is usually much smaller than that of the cytosol. On the other hand, a buffering effect results from the fact that part of the stored calcium is bound to proteins. It is worthwhile including this binding in future extensions of the model. Another aspect worth being considered in the future is the role of the calcium–proton exchanger operative in the ER membrane of many cells [22] and the binding of protons to proteins.

The system is characterized by multistationarity in that three steady states are obtained for appropriate parameter values. We have carried out a local stability analysis of these states. Depending on the parameter values, one or two of these states turn out to be stable. Moreover, the stability analysis has been very helpful for finding parameter values for which limit-cycle oscillations can be expected. We have analysed the transitions between different types of dynamic behaviour upon changes of parameter values, leaving a more detailed bifurcation analysis to a sequel paper.

The oscillations obtained on the basis of our model have the typical spike-like shape found in experiments. The oscillation period of some seconds to some minutes and the amplitude of the calcium oscillations of about 1.5 μM are in good agreement with experimental values [1,5]. Oscillations of the ER potential have been investigated experimentally to lesser an extent. In these investigations (e.g., [21]), high amplitudes of the transmembrane potential were observed only when the concentrations or permeabilities of counterions were very low. In the in vivo situation characterized by high concentrations and permeabilities, amplitudes are below 10 mV, which is in qualitative agreement with our results. If the anion and cation concentrations are decreased by some factor, our model yields amplitudes larger by about the same factor. A similar effect results when the volume ratio is decreased.

The model describes both the switch between stationary and pulsatile regimes, which serves as a digital signal, and changes in oscillation frequency, which serve as analogue signals [4]. The onset or termination of oscillations can be induced by changing a parameter, for example the rate constant of the ATPase, k_{pump}. Calcium oscillations can indeed be triggered or terminated by addition of thapsigargin, which is a specific inhibitor of the ER Ca^{2+}-ATPase [39]. Both effects can be simulated by our model when k_{pump} is gradually decreased beginning with a high value, so that two consecutive Hopf bifurcations occur (see the points P_1 and P_2 in Fig. 8). For the in vivo situation, these transitions are in most cases induced by a change in the maximal channel conductance. $\tilde{g}_{Ca}$, due to an increase in IP_3 concentration, for example. In the diagrams shown in Fig. 4, Fig. 6 and Fig. 8, such a change would correspond to a vertical crossing of the curve a_1 defined by $tr = 0$. For technical reasons, we have preferred changing the parameter k_{pump}, thus crossing that curve horizontally, which gives the same qualitative effect, namely a Hopf bifurcation.

Calcium oscillations as well as other biological oscillations are often referred to as frequency encoded, because their frequencies usually change more significantly than their amplitudes, e.g., upon hormone stimulation (cf. [7]). In our model, the amplitude of the calcium oscillation is fairly constant upon a change of the binding to proteins (cf. Fig. 5A and 9A) or of the volume ratio (cf. Fig. 5A and Fig. 7A, note that the frequency changes by the factor 10 in this case). In contrast, the change in the amplitude of the potential oscillations is more pronounced, in particular upon a change in the binding properties. Importantly, the occurrence of supercritical Hopf bifurcations implies that the amplitude does change considerably near the boundary of the parameter region of oscillatory regimes. So the insensitivity of amplitudes is certainly no dogma (cf. [11]).

In the oscillations obtained by numerical integration of our model equations, peaks of maximal cytosolic calcium concentration correspond to depolarized transmembrane potential values (low absolute values), as should be expected. In contrast, the simulations presented by Jafri and coworkers [11,20] exhibit the puzzling phenomenon that calcium spikes correspond to high transmembrane potential values. This is probably due to a

flaw in the cited papers concerning the sign of the potential difference, which should be negative when defined according to Eq. (4). Positive values can be obtained by changing the ratio of the rate constant of Ca^{2+}-ATPase, k_{pump}, and the calcium conductivity. Although Jafri et al. [20] estimate k_{pump} to be about 250 s^{-1}, they use a value of 20.2 s^{-1}. Interestingly, the steady-state value of the potential difference is negative when calculated with the former value and positive with the latter value of k_{pump}.

The model can easily be extended by inclusion of magnesium. This cation would enter the quasi-electroneutrality condition in a similar way as the monovalent counterions with obvious modifications because Mg^{2+} is bivalent. Consideration of Mg^{2+} would also allow us to take into account the competition between Ca^{2+} and Mg^{2+} for the Ca^{2+} channel.

Several authors suppose that a permanent calcium entry into the cytosol from outside is necessary for oscillations to arise [7,11,14,19,20]. In our model, we have included neither such an influx nor a calcium flux out of the cell. The results show that oscillations can arise all the same. We think that this is not in contradiction of the above-mentioned view, because the role of these fluxes is played, in our model, by the fluxes of the binding and dissociation of calcium to and from proteins.

Acknowledgements

The financial support for a 6 months stay of M.M. at Humboldt University by the Slovenian Science Foundation is gratefully acknowledged. We would like to thank Drs Roland Glaser, Ingolf Bernhardt, and Thomas Pomorski (Berlin) for helpful discussions.

References

[1] N.M. Woods, K.S.R. Cuthbertson and P.H. Cobbold, Nature 319 (1986) 600.
[2] N.M. Woods, K.S.R. Cuthbertson and P.H. Cobbold, Cell Calcium 8 (1987) 79.
[3] M.J. Berridge, in A. Goldbeter (Editor), Cell to Cell Signalling: From Experiments to Theoretical Models (Academic Press, London, 1989) pp. 449.
[4] M.J. Berridge, Nature 361 (1993) 315.
[5] K.S.R. Cuthbertson, in A. Goldbeter (Editor), Cell to Cell Signalling: From Experiments to Theoretical Models (Academic Press, London, 1989) pp. 435.
[6] F. Ichas, L.S. Jouaville, S.S. Sidash, J.-P. Mazat and E.L. Holmuhamedov, FEBS Lett. 348 (1994) 211.
[7] A. Goldbeter, G. Dupont and M.J. Berridge, Proc. Nat. Acad. Sci. USA 87 (1990) 1461.
[8] G. Dupont, M.J. Berridge and A. Goldbeter, Cell Calcium 12 (1991) 73.
[9] R. Somogyi and J.W. Stucki, J. Biol. Chem. 266 (1991) 11068.
[10] Y.-X. Li and J. Rinzel, J. Theor. Biol. 166 (1994) 461.
[11] M.S. Jafri and B. Gillo, Cell Calcium 16 (1994) 9.
[12] R. Heinrich and S. Schuster, The Regulation of Cellular Systems (Chapman and Hall, New York, 1996).
[13] G.W. DeYoung and J. Keizer, Proc. Natl. Acad. Sci. USA 89 (1992) 9895.
[14] G. Dupont and A. Goldbeter, Cell Calcium 14 (1993) 311.
[15] A. Goldbeter, Biochemical Oscillations and Cellular Rhythms (Cambridge University Press, Cambridge, 1996).
[16] H.-D. Jakubke and H. Jeschkeit (Editors), Concise Encyclopedia Chemistry (De Gruyter, Berlin, 1994).
[17] T. Meyer and L. Stryer, Proc. Nat. Acad. Sci. USA 85 (1988) 5051.
[18] T. Meyer and L. Stryer, Ann. Rev. Biophys. Biophys. Chem. 20 (1991) 153.
[19] G. Dupont and A. Goldbeter, in A. Goldbeter (Editor), Cell to Cell Signalling: From Experiments to Theoretical Models (Academic Press, London, 1989) pp. 461-474.
[20] M.S. Jafri, S. Vajda, P. Pasik and B. Gillo, Biophys. J. 63 (1992) 235.
[21] T.J. Beeler, R.H. Farmen and A.N. Martonosi, J. Membrane Biol. 62 (1981) 113.
[22] P. Läuger, Electrogenic Ion Pumps (Sinauer Associates, Sunderland, 1991.
[23] B. Allard, M. Moutin and M. Ronjat, FEBS Lett. 314 (1992) 81.
[24] E.A. Guggenheim, Thermodynamics (North-Holland, Amsterdam, 1950).

[25] S.G. Schultz, Basic Principles of Membrane Transport (Cambridge University Press, Cambridge, 1980).
[26] M. Brumen and R. Heinrich, BioSystems 17 (1984) 155.
[27] A. Werner and R. Heinrich, Biomed. Biochim. Acta 44 (1985) 185.
[28] S. Schuster and J.-P. Mazat, in S. Schuster, M. Rigoulet, R. Ouhabi and J.-P. Mazat (Editors), Modern Trends in Biothermokinetics (Plenum Press, New York, 1993) pp. 33–44.
[29] M. Mazzanti, L.J. Defelice and Y.-M. Liu, J. Physiol. 443 (1991) 307.
[30] S. Risso and L.J. DeFelice, Biophys. J. 65 (1993) 1006.
[31] W.J. Moore, Physical Chemistry (Prentice-Hall, Englewood Cliffs, NJ, 1972).
[32] D.E. Goldman, J. Gen. Physiol. 27 (1943) 37.
[33] E. Heinz, Electric Potentials in Biological Membrane Transport (Springer, Berlin, 1981).
[34] N.B. Standen and P.R. Stanfield, Proc. R. Soc. Lond. B 217 (1982) 101.
[35] L.J. DeFelice, J. Membrane Biol. 133 (1993) 191.
[36] G.D. Smith, J. Wagner and J. Keizer, Biophys. J. 70 (1996) 2527.
[37] W. Hahn, Stability of Motion (Springer-Verlag, Berlin, 1967).
[38] J. Lippincott-Schwartz, in I.M. Arias, J.L. Boyer, N. Fausto, W.B. Jakoby, D.A. Schachter and D.A. Schafritz (Editors), The Liver: Biology and Pathology, 3rd Edn. (Raven Press, New York, 1994).
[39] J.K. Foskett, C.M. Roifman and D. Wong, J. Biol. Chem. 266 (1991) 2778.